



Identification of Repurposed FDA Drugs by Targeting Sclerostin via the Wnt Pathway for Alveolar Bone Formation

Pradeep K. Yadalam¹ Raghavendra V. Anegundi¹ Ramya Ramadoss² Deepti Shrivastava³
Awsaf Murdhi Alruwaili⁴ Muhammad Faheemuddin⁵ Kumar Chandan Srivastava^{6,7}

¹ Department of Periodontics, Saveetha Dental College, Saveetha Institute of Medical and Technical Sciences, Saveetha University, Chennai, Tamil Nadu, India

² Department of Oral Pathology and Oral Biology, Saveetha Dental College and Hospitals, Saveetha Institute of Medical and Technical Sciences, Saveetha University, Chennai, India

³ Periodontics Division, Preventive Dentistry Department, College of Dentistry, Jouf University, Sakaka, Saudi Arabia

⁴ College of Dentistry, Jouf University, Sakaka, Saudi Arabia

⁵ Department of Prosthodontics and Implantology, College of Dentistry, King Faisal University, Al-Ahsa, Saudi Arabia

⁶ Oral Medicine and Maxillofacial Radiology Division, Department of Oral and Maxillofacial Surgery and Diagnostic Sciences, College of Dentistry, Jouf University, Sakaka, Saudi Arabia

⁷ Department of Oral Medicine and Radiology, Saveetha Dental College, Saveetha Institute of Medical and Technical Sciences, Saveetha University, Chennai, Tamil Nadu, India

Address for correspondence Ramya Ramadoss, MDS, PhD, Department of Oral Pathology and Oral Biology, Saveetha Dental College and Hospitals, Saveetha Institute of Medical and Technical Sciences, Saveetha University, Chennai, 600077, India (e-mail: drramya268@gmail.com).

Deepti Shrivastava, B.D.S, M.D.S, Cert Oral & Maxillofacial Implantologist, MFD RCSI (Ireland), MFDS RCPS (Glasg), IFWDC (USA), Periodontics Division, Preventive Dentistry Department, College of Dentistry, Jouf University, Sakaka 72345, Saudi Arabia (e-mail: sdeepti20@gmail.com).

Eur J Gen Dent

Abstract

Objective Natural wingless-related integration site (Wnt) pathway antagonist sclerostin (SOST) has attracted much attention because unusual bone illnesses characterized by the increased bone mass result from its absence of action. The Wnt ligand is prevented from attaching to the Frizzled family receptor when SOST is present. In the active destruction complex, -catenin is phosphorylated. -Catenin molecules do not enter the nucleus and are broken down by a proteasome. As a result, Wnt-responsive genes are not activated, which lowers bone formation and raises bone resorption. A humanized monoclonal antibody called romosozumab binds to and inhibits SOST with significant cardiac side effects. As a result, the current study's objective is to find and screen Food and Drug Administration (FDA) medications that target SOST.

Materials and Methods SOST's structure was retrieved from Protein Data Bank (PDB) (ID: 6I6r). Pharmacophore modeling and molecular operating environment-based virtual testing of FDA-approved medicines. Using the Desmond program, docking and molecular dynamics simulations were performed.

Results Our findings revealed medications with FDA approval (ZINC000253387843) Amphotericin B. The stability and receptor–ligand interactions are pretty substantial, as demonstrated by the findings of docking and Molecular dynamics simulations, which

Keywords

- ▶ bone remodeling
- ▶ sclerostin
- ▶ periodontal disease
- ▶ Wnt pathway
- ▶ osteoblast

DOI <https://doi.org/10.1055/s-0043-1777841>.
ISSN 2320-4753.

© 2024. The Author(s).

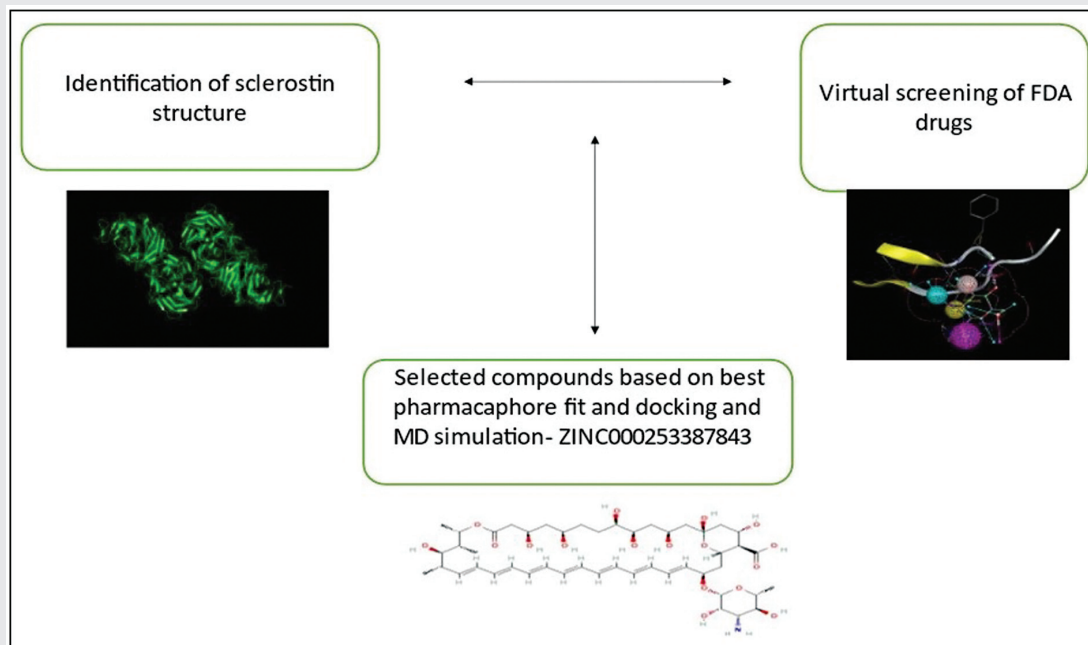
This is an open access article published by Thieme under the terms of the Creative Commons Attribution License, permitting unrestricted use, distribution, and reproduction so long as the original work is properly cited. (<https://creativecommons.org/licenses/by/4.0/>)

Thieme Medical and Scientific Publishers Pvt. Ltd., A-12, 2nd Floor, Sector 2, Noida-201301 UP, India

have a docking score of -7.3 k/mol and root mean square deviation stability at 40 nanoseconds, respectively.

Conclusion The suggested pharmacological therapy shows promise since it uses the Wnt pathway to target the primary bone formation mechanism. However, additional prospective studies are required to apply the available data to clinical practice.

Graphical Abstract



Introduction

Bone is a dynamic tissue that is constantly changing.¹ A phase of resorption of the mineralized matrix by osteoclasts precedes a bone formation phase by osteoblasts in a time- and space-dependent manner to maintain skeletal integrity. The discovery of new therapeutic targets for treating low bone mass and preventing fractures has been made possible by a better knowledge of the regulatory processes involved in bone remodeling.² One of these is the canonical Wnt pathway (wingless-related integration site), which promotes bone formation and prevents bone resorption. Natural Wnt pathway antagonist sclerostin (SOST) has drawn a lot of interest because unusual bone illnesses characterized by increased bone mass result from its absence of action.

Mesenchymal stem cells are committed to the osteoblastic lineage and undergo various stages of osteoblast formation as a result of the Wnt signaling pathway. The pathway activation also inhibits osteoclast bone resorption by increasing osteoblast and osteocyte production of osteoprotegerin ((a decoy receptor for Receptor activator of NF- κ B (RANK-Ligand)). Wnt

molecules stimulate osteoclast progenitor proliferation but hinder differentiation. Without Wnt ligand, a destruction complex phosphorylates β -catenin, directing it for ubiquitination and proteasome degradation. Wnt ligands block the destruction complex by binding to the Frizzled and low-density lipoprotein receptor-related protein 5 and 6 (LRP5/6) co-receptors.³ β -catenin accumulates, translocate to the nucleus, and activates bone-forming genes. Wnt ligands can also activate noncanonical Wnt pathways, but they accelerate bone resorption. Natural antagonists of the Wnt pathway include Dickkopf 1 (DKK1) and SOST.⁴ SOST binds to the LRP5/6 co-receptor to inhibit bone growth. Cells in mineralized matrices, mature osteocytes, and hypertrophic chondrocytes or cementocytes are the principal producers of SOST. Additionally, it is expressed in nonmineralized diseased cells as well as the kidney, liver, heart, and carotid arteries. Interleukin-6 cytokines, parathyroid hormone, and mechanical stress all affect how much SOST is expressed in osteocytes. SOST is a therapeutic target for promoting bone growth in osteoporosis or other bone illnesses since it generates high bone mass diseases like sclerosteosis or Van Buchem disease.⁵

The Wnt signaling pathway is essential for tissue homeostasis, embryonic organogenesis, and wound healing. By enhancing osteoblast development, the Wnt/catenin pathway promotes osteoblastogenesis, and Receptor activator of NF- κ B (RANK)/Receptor activator of NF- κ B Ligand (RANKL) signaling prevents osteoclastogenesis.⁶ There are canonical (involve β -catenin) and noncanonical Wnt signaling pathways. In adults, bone homeostasis and remodeling depend on the Wnt–catenin. A sequence of cellular modifications brought on by the binding of a Wnt ligand to a specific Frizzled family receptor (G protein-coupled receptor)⁷ and an LRP5/6 co-receptor restrict the action of the destruction complex, which is made up of axin and other proteins like dishevelled, adenomatous polyposis coli, and Glycogen-synthase kinase-3 (GSK3) phosphates β -catenin.⁸ When blocked, it cannot phosphorylate β -catenin. Unphosphorylated β -catenin is not broken down, leading to cell accumulation. They bind to the T-cell/lymphoid enhancer factor once within the nucleus, activating genes that cause bone formation in response to Wnt. The Wnt ligand is prevented from attaching to the Frizzled family receptor when SOST is present. In the active destruction complex, β -catenin is phosphorylated. Phosphorylated β -catenin is digested by a proteasome. Molecules of β -catenin do not go into the nucleus. As a result, Wnt-responsive genes are not activated, which lowers bone formation and raises bone resorption.⁹

On chromosome 17q12–q21, the SOST gene resides. In conditions including sclerosteosis, craniodiaphyseal dysplasia, and Van Buchem disease, SOST gene mutations^{3,5} result in inadequate SOST production. This sparked study on SOST and bone mass. Bone development and deterioration are regulated by SOST. Caspases are activated, which speeds up osteoblastic cell apoptosis,¹⁰ and osteoblast differentiation is inhibited, which reduces bone synthesis in areas where remodeling is not required. Osteocyte SOST secretion is decreased and bone development is accelerated by mechanical forces (loading, exercise),¹¹ bone microtrauma, parathyroid hormone (PTH), and estrogen. The release of SOST is stimulated by Bone morphogenetic proteins (BMP)s 2, 4, 6, glucocorticoids, and calcitriol.¹²

Periodontal disease degrades tooth-supporting tissues through complex pathological processes. They are associated with bacterial biofilm components and host response mechanisms. Periodontitis is the irreversible destructive stage of a persistent bacterial infection, while gingivitis is the reversible inflammatory stage.^{13–17} Untreated periodontitis causes soft tissue and bone degeneration, tooth movement, and eventual tooth loss.

Periodontal regeneration therapy aims to restore the health and function of periodontal tissues. Considerable osseous deficiencies from periodontal disease¹¹ are challenging to restore, and results from bone grafts and guided bone regeneration are inconsistent. According to studies on Wnt and BMP signaling on bone homeostasis, Wnt signal-enhancing drugs may be a viable alternative therapy to prevent bone loss and repair periodontal supporting tissues.¹⁸

The SOST gene encodes SOST, a secreted glycoprotein. SOST, generated by osteocytes, suppresses osteoblast development and bone synthesis. Although SOST decreases bone formation,

the exact mechanism by which SOST decreases bone formation is obscure. Still, studies have shown that it inhibits Wnt/ β -catenin signaling, impairing osteoblast differentiation and activation. SOST inhibition increased alveolar bone volume and architecture in rats with alveolar bone loss. Anti-sclerostin monoclonal antibody (Scl-Ab) might be a bone anabolic agent for improving alveolar crest height and alveolar bone mass in periodontitis with estrogen deficiency osteopenia. Upon investigational periodontitis, Scl-Ab restored bone mass.¹⁹

In a rat model of postmenopausal osteoporosis, a neutralizing murine Scl-Ab restores bone growth, mass, and strength. This is also demonstrated in rat and nonhuman monkey models. Most studies link osteoporosis and periodontitis. Additional well-controlled studies are needed to clarify the relationship between systemic and oral bone loss and whether dentists can provide an early osteoporosis warning. Regular oral hygiene and bone density exams can prevent osteoporosis and periodontitis. Unlike alendronate,²⁰ romosozumab^{21–24} increases cardiovascular risk by 30%. Animal research has steadily proven SOST's protective role in the cardiovascular system, despite romosozumab's increased cardiovascular risk.

Several monoclonal antibodies have been created that target the human version of SOST and block its function. Romosozumab is a humanized monoclonal antibody that binds and blocks SOST, boosting bone formation, and decreasing bone resorption. In postmenopausal osteoporosis, romosozumab increases bone mineral density (BMD) and has moderate-quality evidence. No difference in total Adverse events (AE) and severe AE with romosozumab reinforces the drug's recommendation for osteoporosis treatment. There is strong evidence of cardiovascular events,²¹ serious adverse events, hypersensitivity, malignancy, hyperostosis, and osteoarthritis. Serious adverse effects remain a concern, especially in cardiovascular patients and diabetes.

Repurposed FDA-approved drugs refer to medications that were originally developed and approved for one specific medical use but are later found to be effective for treating different conditions. This process is also known as drug repositioning or drug rediscovery. By repurposing existing drugs, researchers can potentially save time and resources, as the safety and efficacy of these drugs have already been established through the FDA approval process. Repurposing FDA-approved drugs can lead to quicker development of treatments for various diseases and conditions, providing new therapeutic options.²⁵ Hence, the current study aims to identify and screen FDA drugs targeting SOST.

Materials and Methods

Structure Retrieval

The structure of SOST was downloaded from PDB (ID: 6l6r; <https://www.rcsb.org/>). Its structure was refined and minimized by Swiss-PdbViewer (**– Fig. 1**).

Pharmacophore Modeling and Virtual Screening

The PDB structure of SOST has a co-crystallized compound. Molecular Operating Environment was used to construct a pharmacophore model for the selected molecule. (<https://www.chemcomp.com/index.htm>).

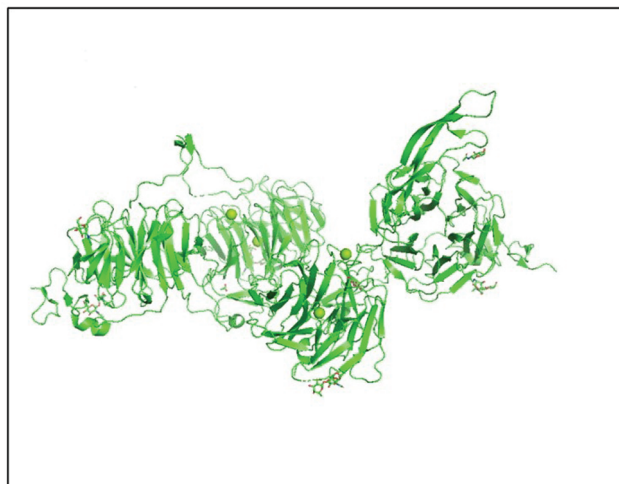


Fig. 1 The image showcases the protein structure of Sclerostin PDB (ID: 6L6r).

After pharmacophore modeling,²⁶ virtual screening²⁷ of FDA-approved drugs was performed via molecular operating environment (MOE) to identify the compounds with features like the pharmacophore model. A library of 1,615 compounds was prepared from the ZINC database. This library includes compounds approved by FDA. Top selected compounds were selected and docked with the receptor SOST.

Molecular Dynamics Simulation

We modeled molecular dynamics for 100 nanoseconds using Desmond (<https://www.schrodinger.com/products/desmond>), a program from Schrödinger LLC.²⁸ To simulate receptor and ligand complexes using molecular dynamics, docking experiments were conducted initially. In static circumstances, ligand-binding states can be predicted by molecular docking studies. Because docking provides a static view of a molecule's binding pose at an RNA active site, it is advantageous. By incorporating Newton's classical equation of motion, MD simulations typically represent atom movements over time. Simulations were used to forecast the ligand-binding status in the physiological environment.

Utilizing Maestro software, the complex refined with reduction of the receptor–ligand complex was performed. The System Builder tool developed each system. The model TIP3P with an orthorhombic box was selected. The simulation used OPLS 2005 force field.²⁷ The models were neutralized by counterions. To imitate physiological circumstances, 0.15 M NaCl was added. The NPT (N, Constant number of particles (atoms or molecules); P: Constant pressure; T, Constant temperature) ensemble with 300 K temperature and 1 atm pressure ran the simulation. We saved the trajectories every 100 PS for analysis and compared the protein and ligand root mean square deviation (RMSD) over time to ensure simulation stability.

Results

The combined pharmacophore model is displayed with matching elements like aromatic rings, hydrogen bond donors, and hydrogen bond acceptors (►Fig. 2). F1 repre-

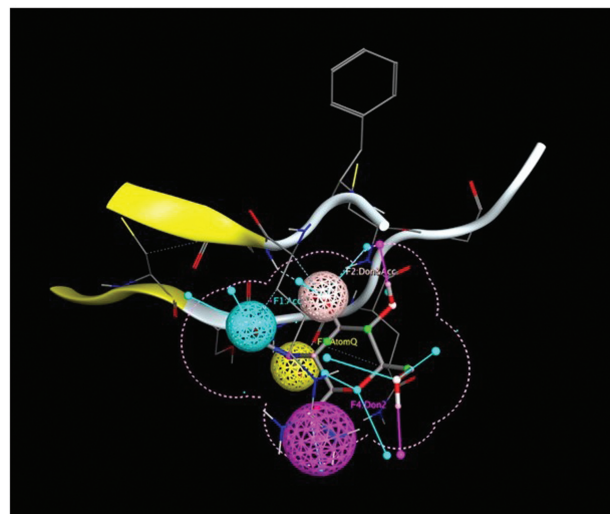


Fig. 2 Ligand-based pharmacophore and selected ligand fit on pharmacophore hypothesis.

Table 1 Table showing binding affinity of top 10 compounds

Molecule	Binding affinity (kcal/mol)
ZINC000253387843	−7.3
ZINC000252286875	−7.1
ZINC000008220909	−6.9
ZINC000003938704	−6.8
ZINC000252286877	−6.8
ZINC000003831490	−6.5
ZINC000003830960	−6.5
ZINC000001540998	−6.5
ZINC000021981454	−6.3
ZINC000084441937	−6.2

sents hydrogen bond acceptors, F2 hydrogen bond donors, and F3 AtomQ and F4 represent hydrogen bond donors and acceptor functional groups, respectively.

In total, 346 hits were found on the base of pharmacophore query using primary filters such as Lipinski's rule of five and restricting the number of rotatable bonds to seven or more to reduce the dataset. Docking of the top 10 compounds was performed.

Top 10 compounds on the base of docking results are shown in ►Table 1.

After analysis, the top three compounds (ZINC000253387843, ZINC000252286875, and ZINC000008220909) were identified as the most active molecules. 2D and 3D interactions of the three bests are shown in ►Fig. 3A–C.

Molecular Dynamics Simulation

►Fig. 4 shows ligand-bound protein C-α atom RMSD values over time. The RMSD plot showed that SOST–ZINC000253387843 proteins consolidated at 10 nanoseconds (►Fig. 4A). After then, RMSD variations stay within 1.0 for the

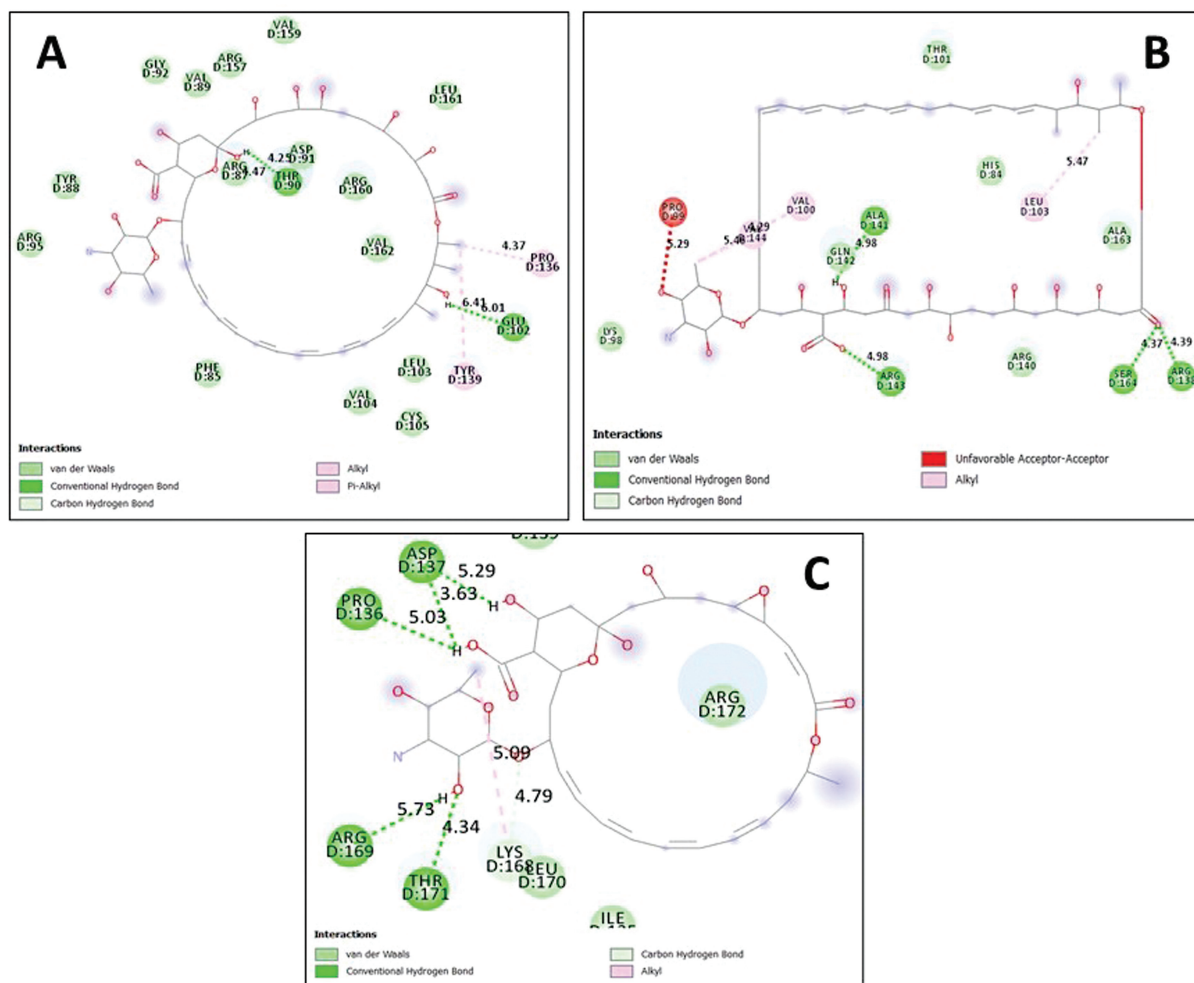


Fig. 3 Interactions. (A) ZINC000253387843, (B) ZINC000252286875, and (C) ZINC000008220909 with sclerostin showing interacting residues and type of interactions.

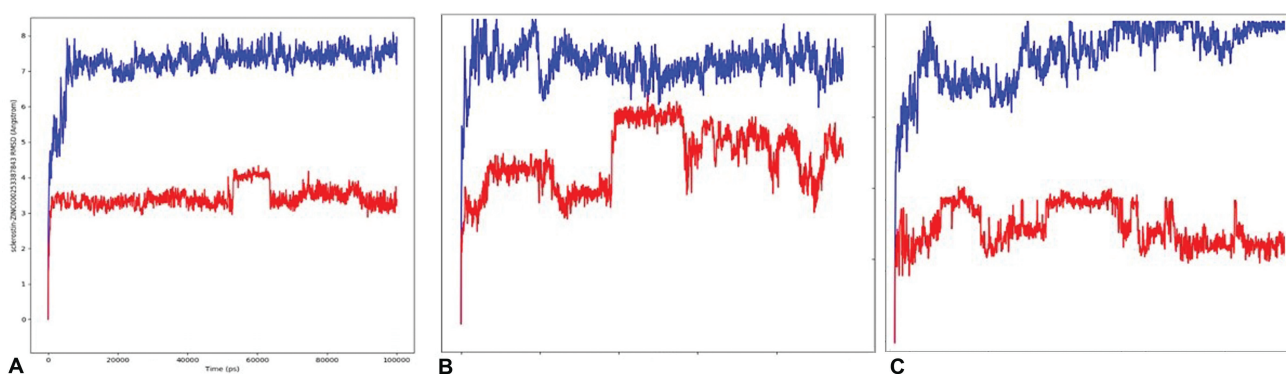


Fig. 4 Root mean square deviation (RMSD) of the C α atoms of proteins and the ligands. (A) Sclerostin–ZINC000253387843, (B) Sclerostin–ZINC000252286875, and (C) Sclerostin–ZINC000008220909 with time. The (left) y-axis shows the variation of RMSD through time. Blue, protein; ligand, red.

simulation, which is good. Ligand RMSD values varied within 1.0 Angstrom up to 55 nanoseconds, turned in ligand mode, remained steady at 65 nanoseconds, and remained unchanged throughout the test.

The RMSD plot of the SOST–ZINC000252286875 demonstrates that the complex settled at 40 nanoseconds

(**Fig. 4B**). The variability in RMSD values for protein after that maintains within 1.5 all through the simulated period. Up to 100 nanoseconds, the RMSD values of ligands varied within 2.0 Angstrom. According to the RMSD plot, the proteins in the complex SOST–ZINC000008220909 obtained stability at 20 nanoseconds (**Fig. 4C**). Following that,

changes in RMSD values remain within 1.0 during the simulation period. Ligand RMSD values vary by up to 100 nanoseconds within 2.0 Angstrom. This suggests that during the simulation time, the ligand retained the binding sites.

►Fig. 5A–C shows the root mean square fluctuation (RMSF) value for the proteins that are associated with the ligand. The molecules with higher peaks are found in the loop regions or N- and C-terminal zones, according to MD trajectories (►Fig. 5). The permanence of ligand binding to the protein is shown by low RMSF values of the binding site residue.

SOST-secondary ZINC000253387843's structure components were determined to be present in proportions of 43.83% overall, 0.00% for Helix, and 43.83% for Strand, respectively (►Fig. 6A). The helix and strand percentages for SOST-ZINC000252286875 were 0.01 and 39.65%, respectively (►Fig. 6B). SSE as a whole was 39.66%. The overall secondary structural components were found to be 37.22%, while the percentages of Helix and Strand in SOST-ZINC000008220909 were 0.00 and 37.22, respectively (►Fig. 6C).

As seen in ►Fig. 7, using MD, the majority of relevant ligand–protein interactions are hydrogen bond connections. Regarding interactions between H-bonds, ARG_87, THR_90, GLU_102, TYR_139, and ARG_160 are the most important for the SOST-ZINC000253387843 complex (►Fig. 7A). GLN_142 and ARG_143 are vital for H-bonds in SOST-ZINC000252286875 (►Fig. 7B). ARG_172 is most crucial as H-bonds for SOST-ZINC000008220909 (►Fig. 7C). The stacked bar

charts were standardized over the trajectory; for instance, a value of 1.0 denotes that the particular interaction was maintained for 100% of the simulation time. Values above 1.0 are possible due to the possibility of some protein residues forming multiple interactions of the same subtype with the ligand.

The radius of gyration (Rg) refers to how atoms in a protein are distributed around its axis (►Fig. 8). The identification of various polymer types, including proteins, is made easier with the use of this conceptual notion. Calculating Rg and distance are the two most crucial indicators for predicting the structural activity of a macromolecule. A conformational shift occurs when a ligand/lead molecule binds to a protein, which alters the Rg. A sophisticated computer method for calculating the Rg can be used to track a protein's compactness, which is directly related to the rate of folding of a protein.

Discussion

Wnt/-catenin signaling system participates in proliferation, differentiation, apoptosis, migration, invasion, and tissue homeostasis. SOST, an osteocyte-secreted protein, inhibits bone formation and promotes bone resorption by binding to LRP5/6 co-receptors.¹¹

The current study utilized Desmond for MD simulations. Desmond is a popular choice for MD simulations due to its exceptional performance, precision, user-friendliness, and scalability. It incorporates advanced force fields and seamless

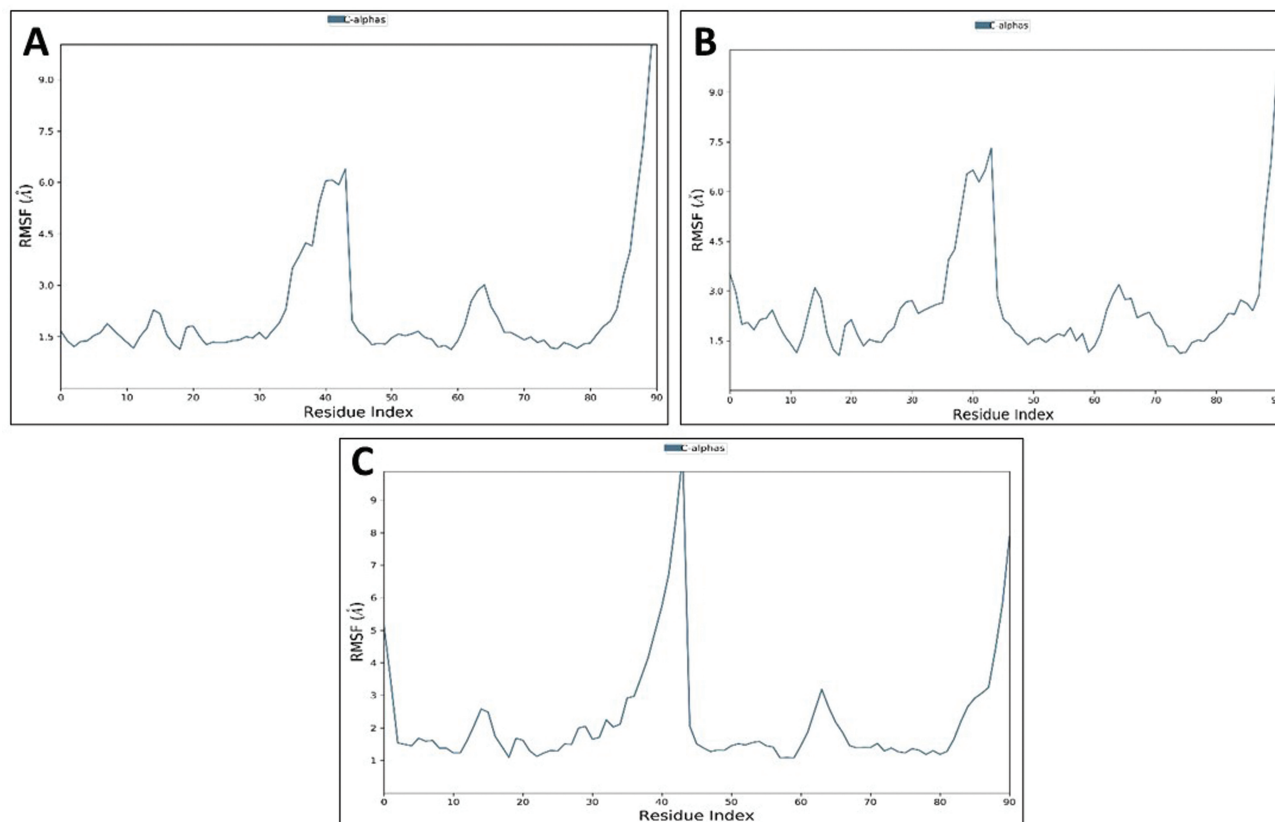


Fig. 5 Residue-wise root mean square fluctuation (RMSF) of protein complexes. (A) Sclerostin-ZINC000253387843, (B) Sclerostin-ZINC000252286875, and (C) Sclerostin-ZINC000008220909.

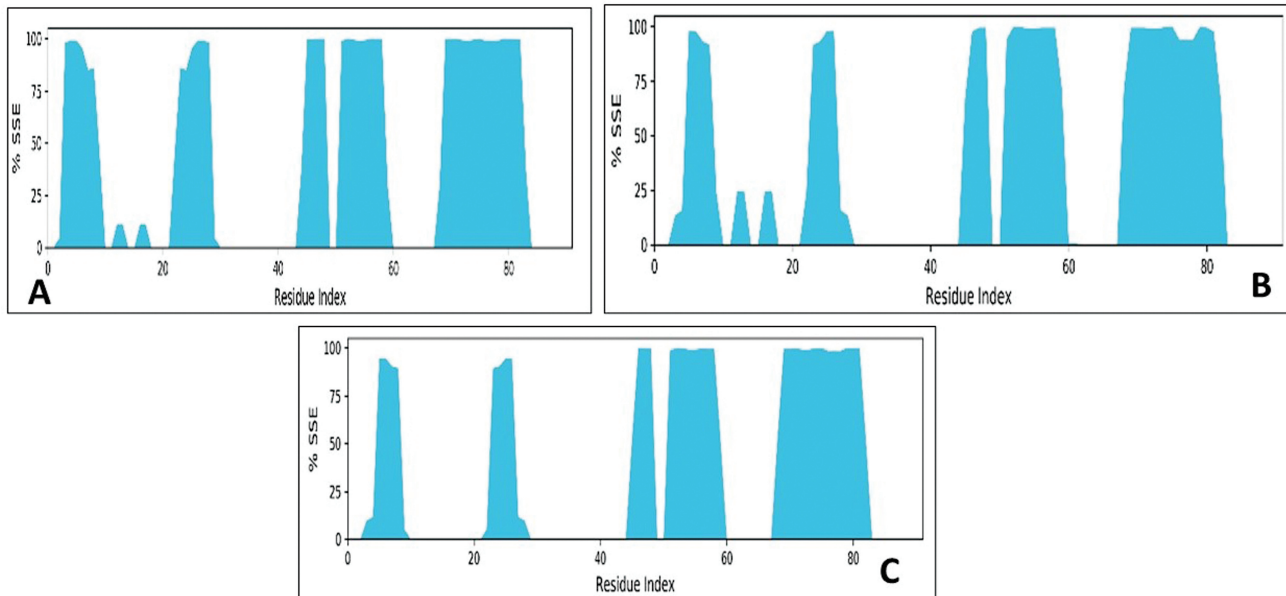


Fig. 6 Protein secondary structure element distribution by residue index throughout the protein structures complexed with ligand. (A) Sclerostin-ZINC000253387843, (B) Sclerostin-ZINC000252286875, and (C) Sclerostin-ZINC00008220909). Red columns indicate α -helices, and blue columns indicate β -strands.

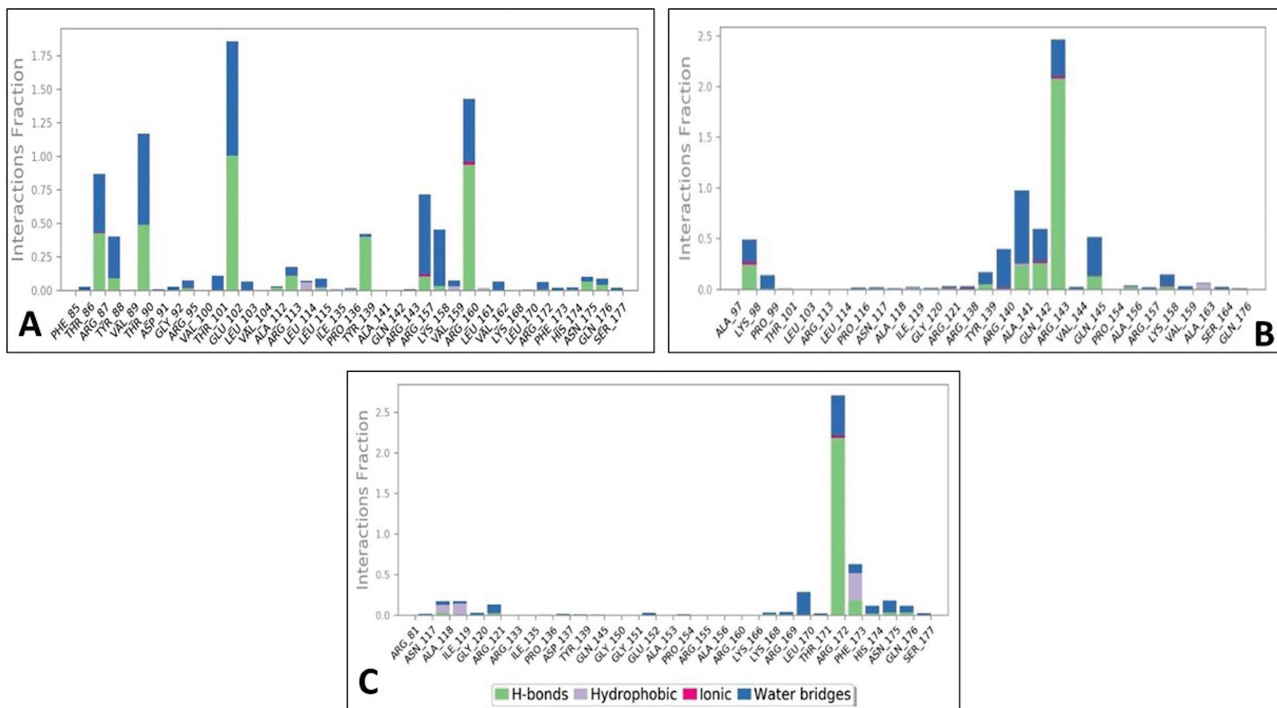


Fig. 7 Protein-ligand contact histogram (protein structures complexed with [A] Sclerostin-ZINC000253387843, [B] Sclerostin-ZINC000252286875, and [C] Sclerostin-ZINC00008220909). H-bond, hydrogen bond.

integration with other tools, making it a reliable and efficient option for researchers studying biological molecules.²⁹

The *SOST* gene was first recognized as pathogenic in sclerosteosis and Van Buchem disease. *SOST* binds LRP5/6 co-receptors, limiting bone growth and boosting bone resorption. Mass spectrometry detected four disulfide links in *SOST*. Disulfide bonds C1eC4 (Cys⁵⁶eCys¹¹⁰), C2eC5 (Cys⁸¹

eCys¹⁴¹), C3eC6 (Cys⁸⁵eCys¹⁴³), and C0eC00 (Cys⁷⁰eCys¹²⁴) define the cystine knot pattern.¹⁰

Muthusamy et al found small compounds targeting *SOST*'s loop 2 domain.³⁰ They found nine small compounds with high predicted binding affinity using web resources for loop 2. Yoon et al³¹ used computational molecular docking to identify probable herbal drugs that would target loop 2 and

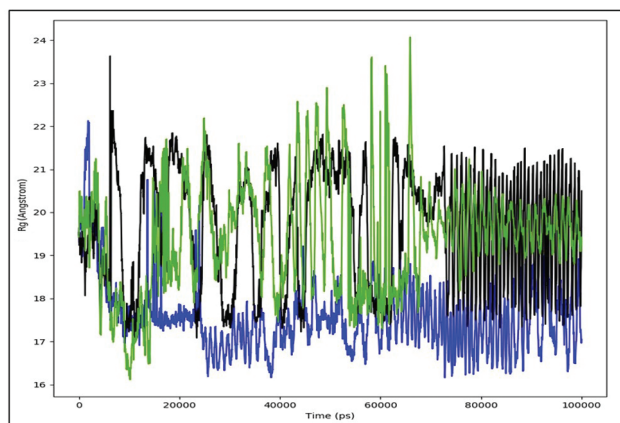


Fig. 8 Radius of gyration calculated for three targets bound with ligand. (Blue, Sclerostin–ZINC000253387843, black: Sclerostin–ZINC000252286875, and green: Sclerostin–ZINC000008220909). Rg, radius of gyration.

act as stimulators of bone growth. Their virtual screening trials discovered a collection of aryl-containing herbal medicines. These compounds displayed high predicted binding affinities, indicating that they can interact strongly and precisely via π – π stacking interactions with specific aromatic amino acid residues. Choi et al.³² used a virtual screening procedure based on pharmacophores to find small-molecule inhibitors that target the LRP5/6e–SOST interaction—based on the results of the virtual screening method’s structure-based virtual screening (19 candidates). Similarly, our pharmacophore virtual screening study identified the top 10 compounds from FDA-approved drugs.

Romozumab triples cardiovascular risk compared with alendronate. Antibodies bind SOST loops 2 and 3. Loop 2 but not loop 3 contributed to SOST’s cardiovascular protective effect, indicating that reducing loop 3’s expressions may promote bone formation without boosting cardiovascular risk.⁶ Our study docked with loop 3, specifically from FDA-approved drugs, to reduce the risk further.

Patient compliance is essential for any long-term drug usage. While some people prefer injections, others prefer oral administration. Due to their aversion to injections, patients do not obtain the necessary medication, which results in less effective treatment. Only being injected, monoclonal antibodies and aptamer medications decrease treatment compliance in individuals who prefer oral therapy, lowering overall treatment efficacy. Therefore, by providing another therapeutic alternative, the development of oral FDA-approved drug small-molecule inhibitors targeting SOST will address the demands of patients.⁶

Numerous FDA-approved drugs have been investigated for their potential to inhibit the Wnt pathway involved in bone formation and target SOST. Denosumab, a monoclonal antibody countering RANKL, is prescribed for osteoporosis and bone metastases; nevertheless, it may entail adverse effects like hypocalcemia and skin reactions. Bisphosphonates, including Alendronate and Risedronate, indirectly influence the Wnt pathway by reducing bone resorption. However, they are

associated with potential drawbacks such as gastrointestinal discomfort and the rare risk of atypical femur fractures. Teriparatide, a promoter of osteoblast activity, can impact the Wnt pathway, although extended use may raise concerns. Raloxifene, a selective estrogen receptor modulator, also plays a role in the Wnt pathway, yet it may come with side effects, including blood clots and hot flashes. However, the use of these drugs for bone-related conditions necessitates careful consideration of potential adverse effects, especially with long-term treatment regimens.³³

Our results identified FDA-approved drugs (ZINC000253387843). Amphotericin B (<https://pubchem.ncbi.nlm.nih.gov/>) is highly active against several fungi. *Candida*, *Histoplasma*, *Coccidioides immitis*, *Streptomyces natalensis*, or *Streptomyces chattanoogaensis*. Amphotericin B (<https://pubchem.ncbi.nlm.nih.gov/>) an amphoteric, macrolide, antifungal is highly active against several fungi including *Candida*, *Histoplasma*, *Coccidioides immitis*, *Streptomyces natalensis*, or *Streptomyces chattanoogaensis*. It is typically used for fungal infections. Amphotericin B and azoles target ergosterol in fungal cytoplasmic membranes. Amphotericin B is an antifungal antibiotic produced by the bacterium, *Streptomyces nodosus*. It has a molecular weight of 924.1 and molecular formula of $C_{47}H_{73}NO_{17}$ and rotatable bond count of 3, and topological polar surface area of 320 \AA^2 . Most individuals who receive IV amphotericin B encounter potentially severe adverse effects during treatment. Conventional IV amphotericin B causes acute infusion responses (fever, chills, headache, nausea, vomiting) and nephrotoxicity. In this periodontal bone regeneration, amphotericin B in a reduced dose helps bone formation by inhibiting SOST. Local applications lead to reduced SOST activity and induce bone formation.

Docking and MD simulation results show that the stability and receptor–ligand interactions are very significant with a docking score of -7.3 k/mol and RMSD stability at 40 nanoseconds and can be considered for usage for regenerating bone in periodontal diseases.

In this study, a selection of FDA-approved drugs with the potential for targeting SOST was determined using robust computational techniques. However, the translation of these findings into clinical applications necessitates further scrutiny. Validation through in vitro and in vivo experiments is imperative to confirm the safety and effectiveness of these identified drug candidates. Moreover, a rigorous evaluation of the compounds’ specificity and selectivity is essential.

To progress this pharmacological approach, there is a need for subsequent research focused on refining drug delivery methods, with a particular emphasis on enhancing oral administration to improve patient compliance. Furthermore, considering the known concerns associated with existing treatments, it is imperative to conduct a thorough assessment of the impact of these repurposed drugs on cardiovascular health. The realization of the clinical potential inherent in these findings will depend on collaborative endeavors between the realms of computational biology and experimental pharmacology. After successful in vitro studies, future animal studies should be planned.

Conclusion

In conclusion, this study identified FDA-approved drugs, particularly Amphotericin B, that exhibits high potential for targeting SOST through the Wnt pathway, thus promoting alveolar bone formation. The comprehensive pharmacophore modeling, virtual screening, and molecular dynamics simulations provided valuable insights into the interactions and stability of these compounds. While the suggested pharmacological therapy shows promise, further prospective studies are warranted to translate these findings into clinical practice. This research opens new avenues for periodontal regeneration, with the potential to address the complex challenges of bone remodeling and diseases such as periodontitis.

Conflict of Interest

None declared.

References

- Brent MB, Brüel A, Thomsen JS. Anti-sclerostin antibodies and abaloparatide have additive effects when used as a countermeasure against disuse osteopenia in female rats. *Bone* 2022; 160:116417
- Ramli FF, Chin K-Y. A review of the potential application of osteocyte-related biomarkers, fibroblast growth factor-23, sclerostin, and Dickkopf-1 in predicting osteoporosis and fractures. *Diagnostics (Basel)* 2020;10(03):145
- Balemans W, Van Den Ende J, Freire Paes-Alves A, et al. Localization of the gene for sclerosteosis to the Van Buchem disease-gene region on chromosome 17q12-q21. *Am J Hum Genet* 1999;64(06):1661-1669
- Hu B, Li Y, Wang M, et al. Functional reconstruction of critical-sized load-bearing bone defects using a Sclerostin-targeting miR-210-3p-based construct to enhance osteogenic activity. *Acta Biomater* 2018;76:275-282
- Van Hul W, Balemans W, Van Hul E, et al. Van Buchem disease (hyperostosis corticalis generalisata) maps to chromosome 17q12-q21. *Am J Hum Genet* 1998;62(02):391-399
- Yu S, Li D, Zhang N, et al. Drug discovery of sclerostin inhibitors. *Acta Pharm Sin B* 2022;12(05):2150-2170
- Yan Y, Tang D, Chen M, et al. Axin2 controls bone remodeling through the β -catenin-BMP signaling pathway in adult mice. *J Cell Sci* 2009;122(Pt 19):3566-3578
- Ke HZ, Richards WG, Li X, Ominsky MS. Sclerostin and Dickkopf-1 as therapeutic targets in bone diseases. *Endocr Rev* 2012;33(05):747-783
- Witcher PC, Miner SE, Horan DJ, et al. Sclerostin neutralization unleashes the osteoanabolic effects of Dkk1 inhibition. *JCI Insight* 2018;3(11):e98673
- Sutherland MK, Geoghegan JC, Yu C, et al. Sclerostin promotes the apoptosis of human osteoblastic cells: a novel regulation of bone formation. *Bone* 2004;35(04):828-835
- Shu R, Bai D, Sheu T, et al. Sclerostin promotes bone remodeling in the process of tooth movement. *PLoS ONE* 2017;12(01):e0167312
- Li X, Ominsky MS, Niu QT, et al. Targeted deletion of the sclerostin gene in mice results in increased bone formation and bone strength. *J Bone Miner Res* 2008;23(06):860-869
- Qi J, Liu E, Guo Y-F, et al. Association between periodontal disease and osteoporosis in postmenopausal women: a protocol for systematic review and meta-analysis. *BMJ Open* 2021;11(09):e049277
- Hong S-J, Yang B-E, Yoo D-M, Kim S-J, Choi H-G, Byun S-H. Analysis of the relationship between periodontitis and osteoporosis/fractures: a cross-sectional study. *BMC Oral Health* 2021;21(01):125
- Esfahanian V, Shamami MS, Shamami MS. Relationship between osteoporosis and periodontal disease: review of the literature. *J Dent (Tehran)* 2012;9(04):256-264
- Martínez-Maestre MÁ, González-Cejudo C, Machuca G, Torrejón R, Castelo-Branco C. Periodontitis and osteoporosis: a systematic review. *Climacteric* 2010;13(06):523-529
- Liao C, Ou Y, Wu Y, Zhou Y, Liang S, Wang Y. Sclerostin inhibits odontogenic differentiation of human pulp-derived odontoblast-like cells under mechanical stress. *J Cell Physiol* 2019;234(11):20779-20789
- Liu M, Kurimoto P, Zhang J, et al. Sclerostin and DKK1 inhibition preserves and augments alveolar bone volume and architecture in rats with alveolar bone loss. *J Dent Res* 2018;97(09):1031-1038
- Yao Y, Kauffmann F, Maekawa S, et al. Sclerostin antibody stimulates periodontal regeneration in large alveolar bone defects. *Sci Rep* 2020;10(01):16217
- Brown JP, Prince RL, Deal C, et al. Comparison of the effect of denosumab and alendronate on BMD and biochemical markers of bone turnover in postmenopausal women with low bone mass: a randomized, blinded, phase 3 trial. *J Bone Miner Res* 2009;24(01):153-161
- Lv F, Cai X, Yang W, et al. Denosumab or romosozumab therapy and risk of cardiovascular events in patients with primary osteoporosis: Systematic review and meta-analysis. *Bone* 2020; 130:115121
- Saag KG, Petersen J, Brandi ML, et al. Romosozumab or alendronate for fracture prevention in women with osteoporosis. *N Engl J Med* 2017;377(15):1417-1427
- Minisola S. Romosozumab: from basic to clinical aspects. *Expert Opin Biol Ther* 2014;14(09):1225-1228
- Cosman F, Crittenden DB, Adachi JD, et al. Romosozumab treatment in postmenopausal women with osteoporosis. *N Engl J Med* 2016;375(16):1532-1543
- Sahoo BM, Ravi Kumar BVV, Sruti J, Mahapatra MK, Banik BK, Borah P. Drug repurposing strategy (DRS): emerging approach to identify potential therapeutics for treatment of novel coronavirus infection. *Front Mol Biosci* 2021;8:628144
- Ferreira LG, Dos Santos RN, Oliva G, Andricopulo AD. Molecular docking and structure-based drug design strategies. *Molecules* 2015;20(07):13384-13421
- Rasheed MA, Iqbal MN, Saddick S, et al. Identification of lead compounds against Scm (fms10) in *Enterococcus faecium* using computer aided drug designing. *Life (Basel)* 2021;11(02):77
- Hildebrand PW, Rose AS, Tiemann JKS. Bringing molecular dynamics simulation data into view. *Trends Biochem Sci* 2019;44(11):902-913
- Salo-Ahen OM, Alanko I, Bhadane R, et al. Molecular dynamics simulations in drug discovery and pharmaceutical development. *Processes (Basel)* 2020;9(01):71
- Muthusamy K, Mohan S, Nagamani S, Kesavan C. Identification of novel small molecules that bind to the loop2 region of sclerostin - an in silico computational analysis. *Physiol Res* 2016;65(05):871-878
- Yoon W, Saenjum C, Ruangsuriya J, Jiranusornkul S. Discovery of potential sclerostin inhibitors from plants with loop2 region of sclerostin inhibition by interacting with residues outside Pro-Asn-Ala-Ile-Gly motif. *J Biomol Struct Dyn* 2020;38(05):1272-1282
- Choi J, Lee K, Kang M, Lim S-K, Tai No K. In silico discovery of quinoxaline derivatives as novel LRP5/6-sclerostin interaction inhibitors. *Bioorg Med Chem Lett* 2018;28(06):1116-1121
- Chandra A, Rajawat J. Skeletal aging and osteoporosis: mechanisms and therapeutics. *Int J Mol Sci* 2021;22(07):3553